JoCoSiR
Journal of Computer Science Research

ISSN 2986-2337 (Online)

Performance Analysis of Histogram Equalization and Color Balance for Underwater Image Restoration

Khairunnisa Samosir

Program Studi Ilmu Komputer, Fakultas Teknik, Universitas Graha Nusantara, Padangsidimpuan, Indonesia
email: khairunnisasamosir01@gmail.com

ARTICLE INFO

Article history:
Received Sep 19, 2026
Revised Oct 9, 2026
Accepted Oct 20, 2026
Available online Oct 26, 2026

ABSTRACT

Underwater images commonly suffer from color casts, low contrast, and reduced visibility caused by wavelength-dependent absorption and scattering of light in water. Histogram Equalization (HE) and Color Balance are two classical spatial-domain techniques frequently applied to mitigate these degradations, yet their comparative performance across different underwater degradation conditions is rarely quantified beyond visual inspection. This study analyzes the performance of per-channel HE and the Simplest Color Balance algorithm on nine real underwater images grouped into three degradation categories: blue-dominant, green-dominant, and dark/turbid. Objective evaluation used Mean Squared Error (MSE), Peak Signal-to-Noise Ratio (PSNR), Shannon entropy, RMS contrast, and a color-cast index, complemented by qualitative visual comparison. Color Balance consistently achieved higher PSNR and lower MSE than HE across all nine images (average PSNR of 16.12, 18.36, and 14.69 dB for the blue, green, and turbid categories versus 11.00, 13.66, and 10.54 dB for HE), indicating more faithful restoration with fewer artifacts. HE produced a greater increase in entropy and contrast and reduced the numerical color-cast index more aggressively, but amplified noise and introduced reddish/magenta artifacts, particularly on the darkest, most compressed image, where PSNR fell to 7.17 dB. Both methods performed best on moderately degraded blue- and green-dominant images and struggled on severely dark, low-bit-depth images, revealing a clear capability boundary for classical spatial-domain restoration. These findings offer practical guidance for selecting or combining HE and Color Balance in underwater image processing pipelines.

IEEE style in citing this article:

K. Samosir, "Performance Analysis of Histogram Equalization and Color Balance for Underwater Image Restoration," *JoCoSiR: Jurnal Ilmiah Teknologi Sistem Informasi*, vol. 4, no. 4, pp. 1-10, 2026.

Copyright: Journal of Computer Science Research (JoCoSiR) with CC BY NC SA license.

1. Introduction

Underwater imaging plays an increasingly important role in marine biology surveys, underwater archaeology, aquaculture and coral-reef health monitoring, subsea infrastructure inspection, and vision-based navigation for autonomous underwater vehicles (AUV) and remotely operated vehicles (ROV) [1]. Unlike images captured in air, light travelling through water is subject to wavelength-dependent absorption and multiple scattering by suspended particles, which together attenuate the red channel far more quickly than the green and blue channels as depth and distance increase [8], [9]. This selective attenuation produces the characteristic blue or green color cast, reduced global contrast, haziness, and loss of fine detail that are commonly observed in raw underwater photographs, and these artifacts substantially degrade the performance of downstream computer-vision tasks such as object detection, species classification, and diver assistance [1].

A wide range of underwater image enhancement and restoration techniques has been proposed to counter these degradations. Physical model-based restoration methods, including variants of the dark channel prior [6] and approaches that explicitly model image blurriness and light absorption [7], attempt to invert the underwater image formation process, but they require accurate estimation of scene depth, transmission, and background light, are computationally demanding, and can fail when their underlying assumptions do not hold [8], [9]. Deep-learning-based enhancement networks have shown strong results on benchmark datasets [11], [12], yet they require large paired training sets and considerable computational resources that are often unavailable for lightweight, real-time, or field-deployed underwater imaging systems. Classical spatial-domain enhancement techniques, particularly Histogram Equalization (HE) and Color Balance, remain attractive alternatives because they are computationally inexpensive, require no training data, and are simple enough to run on embedded hardware; consequently, they continue to be used both as stand-alone enhancement tools and as preprocessing steps inside more elaborate pipelines [10], [15], [16]. This continued reliance on simple, computationally inexpensive classical algorithms is not unique to image processing: comparable reasoning underlies the continued use of classical algorithms such as K-Means clustering for lightweight, interpretable data segmentation in other computational domains, including

ISSN 2986-2337 (Online)

healthcare visit-pattern analytics [23], which similarly favors low-complexity, transparent methods over heavier alternatives whenever the additional complexity is not justified by the task at hand.

Despite their continued popularity, prior comparative studies of HE-family methods on underwater images, including several Indonesian SINTA-indexed studies, generally evaluate performance on a single pooled dataset and report only overall average metrics [18], [19], [22]. It is well documented that underwater degradation manifests very differently depending on water type, depth, and turbidity [1], [17], yet it remains unclear from the existing literature where classical spatial-domain methods such as HE and Color Balance actually succeed and where their capability reaches its limit under specific, clearly separated degradation conditions. Furthermore, many existing comparative studies present only visual before/after illustrations without pairing them with a systematic quantitative evaluation and an explicit discussion of failure cases.

To address this gap, the present study performs a systematic performance analysis of per-channel Histogram Equalization [21] and the Simplest Color Balance algorithm [15] across three explicitly separated underwater degradation categories: blue-dominant, green-dominant, and dark/turbid images. The contribution of this study is threefold: (1) a controlled comparison of HE and Color Balance across distinct, clearly labeled degradation conditions rather than a single pooled dataset; (2) a multi-metric quantitative evaluation combining Mean Squared Error (MSE), Peak Signal-to-Noise Ratio (PSNR), Shannon entropy, RMS contrast, and a color-cast index, in addition to qualitative visual inspection; and (3) an explicit identification and discussion of the conditions under which each method succeeds or fails, including an extreme low-bit-depth failure case that exposes the capability boundary of classical spatial-domain restoration. The objective of this research is to determine the comparative performance and the capability boundary of HE and Color Balance for restoring underwater images under varied, real-world degradation conditions.

2. State of the Art

Research on underwater image quality improvement generally follows two complementary directions: image enhancement, which improves visual quality without explicitly modeling the physics of light propagation, and image restoration, which inverts a physical formation model to recover scene radiance [17]. The construction of the Underwater Image Enhancement Benchmark (UIEB), comprising hundreds of real-world underwater images together with high-quality reference images produced through pairwise comparison, has been a major driver of quantitative, reproducible evaluation in this field and is used as a common testbed by subsequent studies [1].

2.1 Physical Model-Based Restoration

Physical model-based methods estimate the transmission map and background light of a scene and invert the underwater image formation model to recover a haze-free image. The dark channel prior, originally proposed for terrestrial haze removal [6], has been extended and adapted specifically for the underwater domain by incorporating image blurriness and light-absorption cues [7]. More recent work has revised the classical underwater image formation model to more accurately capture wavelength-dependent attenuation [8], and has proposed calibrated restoration pipelines that estimate per-wavelength attenuation coefficients directly from RGBD data [9]. While these physics-driven approaches can achieve high restoration accuracy, they depend on assumptions about scene depth and homogeneous water properties that are frequently violated in real conditions, and their computational cost is considerably higher than that of spatial-domain enhancement techniques.

2.2 Histogram-Based Enhancement and Color Balance

Histogram Equalization redistributes the intensity values of an image so that its cumulative histogram approaches a uniform distribution, thereby increasing global contrast [21]. In the underwater domain, HE has been combined with global-local network structures and compressed-histogram formulations to control over-enhancement [12], and with dehazing formulations guided by a histogram distribution prior [10]. Because naive per-channel HE operates on each color channel independently, it can distort color balance and amplify noise in channels with a narrow original intensity range, a limitation that several red-channel-specific restoration methods were designed to address [14].

Color balance and white-balance techniques instead redistribute or stretch the intensity range of each channel to remove a global color cast. The Unsupervised Colour Correction Method combines RGB channel stretching with an additional HSI-based contrast stretch specifically for underwater scenes [16]. Fusion-based approaches combine a white-balanced input with contrast- and saliency-weighted enhancement maps through multi-scale fusion to improve both color and contrast simultaneously [2], [3]. Weakly supervised color-transfer learning has also been used to correct underwater color casts without requiring paired ground-truth images [13]. Among simple range-stretching techniques, the Simplest Color Balance algorithm clips a small percentage of the most extreme pixel values in each channel and then linearly stretches the remaining range to occupy the full [0, 255] interval

ISSN 2986-2337 (Online)

[15]; because of its simplicity, transparency, and low computational cost, this algorithm is adopted as the Color Balance method evaluated in the present study.

Within the Indonesian research community, several SINTA-indexed studies have directly compared histogram-based enhancement methods on underwater images using MSE and PSNR. Suharyanto and Frieyadie compared HE, Adaptive Histogram Equalization (AHE), and Contrast-Limited Adaptive Histogram Equalization (CLAHE) on images drawn from the UIEB dataset and found that CLAHE achieved better MSE and PSNR than the plain HE and AHE variants [18]. Asri combined CLAHE with a convolutional neural network classifier to jointly improve underwater image quality and downstream classification performance [19]. More recently, Cahyani et al. evaluated a simple preprocessing pipeline consisting of Lab-space white balance, red-channel boosting, and contrast stretching against Retinex and guided-filtering enhancement on the UIEB challenging subset, using the no-reference UIQM metric, and found that the simple preprocessing pipeline outperformed the more elaborate Retinex and guided-filtering methods on the most severely degraded images [22]. Statistical background-light modeling combined with transmission-map optimization has likewise been proposed as a lightweight alternative to full physical restoration [20]. These findings collectively motivate a closer, category-separated comparison between HE and Color Balance, which is the focus of the present study.

2.3 Evaluation Metrics for Underwater Image Quality

Full-reference metrics such as MSE and PSNR require a paired ground-truth image and have been used in several underwater HE-family comparisons [18]; however, true distortion-free reference images are rarely available for real-world underwater captures without specialized calibration targets, a limitation explicitly acknowledged in the construction of the UIEB benchmark [1]. To evaluate images without an available reference, no-reference metrics have been developed specifically for the underwater domain, including the Underwater Color Image Quality Evaluation (UCIQE) metric, which combines chroma, saturation, and contrast into a single index [4], and the Underwater Image Quality Measure (UIQM), which aggregates colorfulness, sharpness, and contrast measures inspired by the human visual system [5]. The evaluation protocol adopted in the present study, which combines MSE/PSNR with entropy, RMS contrast, and a color-cast index, is described in detail in Section 3.

3. Method

This study follows the five-stage research flow illustrated in Figure 1: dataset collection and categorization, preprocessing, application of the two enhancement methods, quantitative and qualitative evaluation, and comparative analysis to identify the capability boundary of each method. Each processing and evaluation step was implemented in Python 3 using OpenCV and NumPy, and every reported figure was computed directly from the image data rather than estimated.

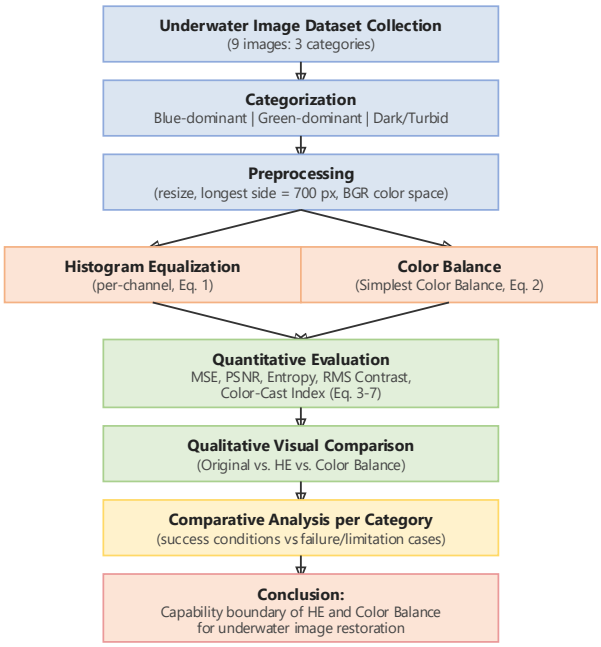


Figure 1. Research flow of this study.

ISSN 2986-2337 (Online)

3.1 Dataset

Because this study specifically evaluates performance under varied degradation conditions rather than a single pooled distribution, nine real underwater photographs were assembled from underwater image processing research collections and organized into three categories of nine, as summarized in Table 1: blue-dominant images typical of deep, clear open water; green-dominant images typical of coastal or algae-rich water; and dark/turbid images representing low-light or high-particulate conditions. All images were resized so that their longest side equaled 700 pixels prior to processing, to keep computation time and figure sizes consistent across the dataset, and were processed in 8-bit BGR color space.

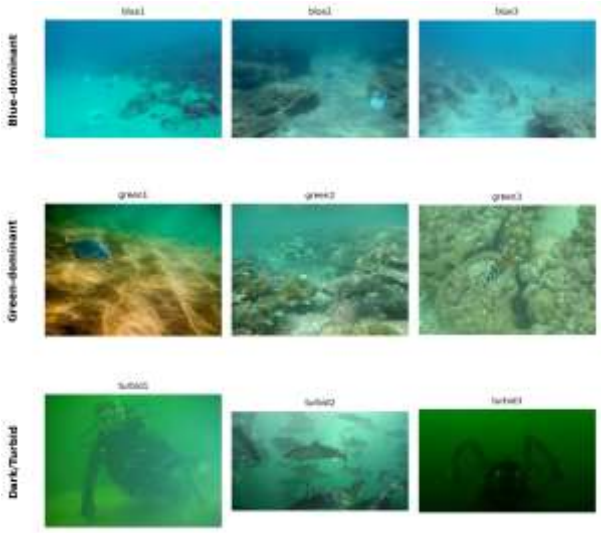


Figure 2. Sample of the nine test images grouped by degradation category.

Table 1. Composition of the underwater image test dataset

Category	No. of Images	Dominant Characteristic	File ID
Blue-dominant	3	Strong blue color cast, hazy	blue1–blue3
Green-dominant	3	Green-teal color cast	green1–green3
Dark/turbid	3	Low light, low visibility, haze	turbid1–turbid3
Total	**9**	—	—

3.2 Histogram Equalization

Histogram Equalization (HE) was applied independently to each of the red, green, and blue channels. For a channel with intensity function f and L possible gray levels, the output g is obtained by mapping each input intensity through the cumulative distribution function (CDF) of that channel, as expressed in Equation (1) and Equation (2):

$$g(x,y) = round[(L-1) \times CDF(f(x,y))] \quad (1)$$

$$CDF(k) = \sum_{i=0}^{k} \frac{n_i}{N} \quad (2)$$

where ni is the number of pixels with intensity i, N is the total number of pixels in the channel, and L = 256. This global per-channel procedure was chosen because it represents the classical, most widely implemented form of Histogram Equalization referenced across the underwater HE literature [18], [21], and it deliberately makes no adjustment for the channel-dependent noise characteristics of underwater images, allowing its inherent strengths and weaknesses to be observed directly.

3.3 Color Balance

Color Balance was implemented using the Simplest Color Balance algorithm [15]. For each channel c, the s/2 % lowest and s/2 % highest intensity values are clipped, and the remaining range is linearly stretched to occupy the full [0, 255] interval, as expressed in Equation (3):

ISSN 2986-2337 (Online)

$$f'_c(x,y) = clip\frac{f_c(x,y) - V_{min,c}}{V_{max,c} - V_{min,c}} \times 255, 0, 255 \quad (3)$$

where Vmin,c and Vmax,c are the s/2-th and (100 − s/2)-th percentile intensity values of channel c. A clip percentage of s = 1% was used uniformly across all nine images, following the default recommendation in the original algorithm [15].

3.4 Evaluation Protocol

A well-documented limitation of underwater image quality assessment is that true, distortion-free scene radiance is generally unavailable for real-world captures without specialized calibration equipment, which is why even large benchmark efforts such as UIEB had to construct reference images through subjective pairwise comparison rather than physical ground truth [1]. Because the nine images used in this study are genuine underwater photographs without a paired radiometric reference, MSE and PSNR were computed between each original (unprocessed) image and its corresponding HE or Color Balance output, following the same original-versus-enhanced comparison protocol used in comparable underwater HE studies [18]. Within this protocol, MSE and PSNR quantify the magnitude of pixel-level modification introduced by each method rather than restoration accuracy against a known-clean reference; a larger modification is not automatically better or worse, which is why MSE/PSNR were interpreted jointly with entropy, RMS contrast, and the color-cast index, and were always read together with the qualitative visual comparison in Section 4.

MSE and PSNR were computed as shown in Equation (4) and Equation (5):

$$MSE = \frac{1}{M \times N}\sum_{x,y}[I(x,y) - I'(x,y)]^2 \quad (4)$$

$$PSNR = 10\, log_{10}(\frac{255^2}{MSE}) \quad (5)$$

where M × N is the total number of pixels and I and I′ denote the original and processed image, respectively, averaged across the three color channels. Shannon entropy, used to quantify information content, is given in Equation (6):

$$H = -\sum_{i=0}^{L-1} p_i\, log_2(p_i) \quad (6)$$

where pi is the normalized histogram frequency of intensity i on the grayscale-converted image. RMS contrast is the standard deviation of the grayscale intensity, and the color-cast index used to summarize channel imbalance is the standard deviation of the three channel means μR, μG, and μB, as given in Equation (7):

$$CCI = std(\mu_R, \mu_G, \mu_B) \quad (7)$$

A lower CCI indicates a more balanced distribution of average intensity across the three color channels, i.e., a weaker residual color cast.

4. Results and Discussion

This section presents the quantitative and qualitative results obtained by applying per-channel Histogram Equalization (HE) and Simplest Color Balance (CB) to the nine-image, three-category dataset described in Section 3, followed by a comparative discussion that identifies the conditions under which each method succeeds or fails.

4.1 Quantitative Results

Table 2 summarizes the average MSE and PSNR obtained for each category, and Table 3 summarizes the average entropy (H), RMS contrast (C), and color-cast index (CCI) before processing and after each method. Table 4 reports the full per-image MSE and PSNR values.

Table 2. Average MSE and PSNR per category

Category	MSE (HE)	PSNR (HE) dB	MSE (CB)	PSNR (CB) dB
Blue-dominant	5516.43	11.00	1601.76	16.12
Green-dominant	2805.94	13.66	1010.93	18.36
Dark/turbid	7034.20	10.54	2644.66	14.69

ISSN 2986-2337 (Online)

Table 3. Average entropy (H), RMS contrast (C), and color-cast index (CCI) per category

Category	H orig	H HE	H CB	C orig	C HE	C CB	CCI orig	CCI HE	CCI CB
Blue	6.42	7.60	7.16	26.04	57.76	44.99	56.09	5.94	31.30
Green	6.91	7.90	7.58	30.95	66.08	49.36	24.34	0.95	17.48
Turbid	6.51	7.69	7.53	26.83	64.23	54.76	35.14	6.83	21.67

Table 4. Per-image MSE and PSNR

Image	Category	MSE (HE)	PSNR (HE)	MSE (CB)	PSNR (CB)
blue1	Blue	8104.34	9.04	1384.75	16.72
blue2	Blue	3334.49	12.90	1571.53	16.17
blue3	Blue	5110.44	11.05	1848.98	15.46
green1	Green	2511.07	14.13	1147.12	17.54
green2	Green	2852.68	13.58	563.43	20.62
green3	Green	3054.05	13.28	1322.25	16.92
turbid1	Turbid	6152.19	10.24	4148.73	11.95
turbid2	Turbid	2468.86	14.21	897.75	18.60
turbid3	Turbid	12481.56	7.17	2887.49	13.53

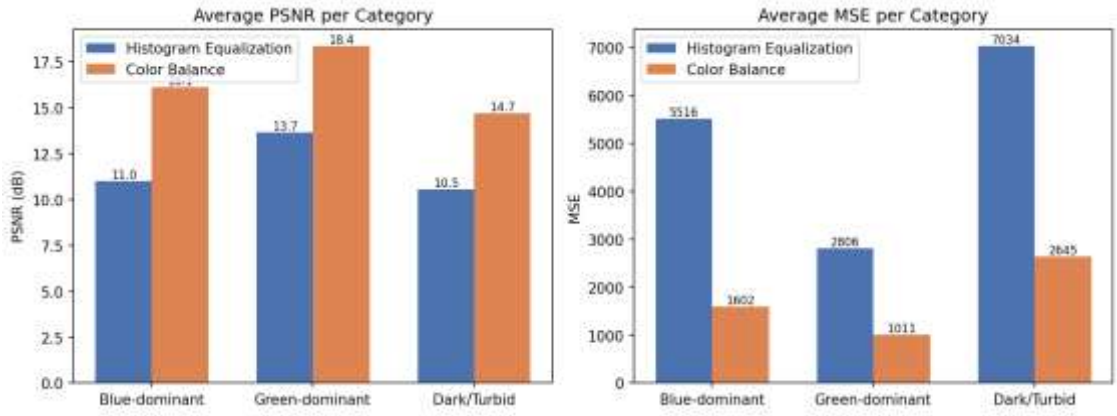


Figure 3. Average PSNR and MSE per category for HE and Color Balance.

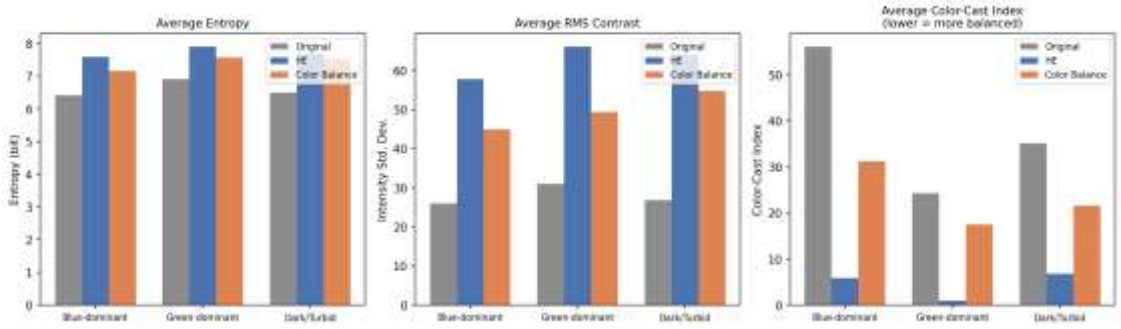


Figure 4. Average entropy, RMS contrast, and color-cast index per category.

Two consistent patterns emerge from Tables 2–4. First, Color Balance achieved a higher PSNR and a lower MSE than HE on all nine test images without exception, and on every one of the three categories on average (Table 2, Figure 3), indicating that Color Balance produced a more faithful, lower-magnitude modification of the original image than HE. Second, HE produced a substantially larger increase in entropy and RMS contrast than Color Balance in every category (Table 3, Figure 4), and reduced the color-cast index far more aggressively than Color Balance — for example, the blue-dominant category dropped from an original CCI of 56.09 to 5.94 after HE, compared with 31.30 after Color Balance. This pattern is consistent with the theoretical property of Histogram Equalization: by forcing each channel's histogram toward a uniform distribution, HE maximizes entropy and numerically equalizes the three channel means almost regardless of the true scene color, whereas Color Balance

ISSN 2986-2337 (Online)

only stretches the existing distribution and therefore leaves a larger residual imbalance when the original color cast is severe [21].

4.2 Qualitative Analysis per Category

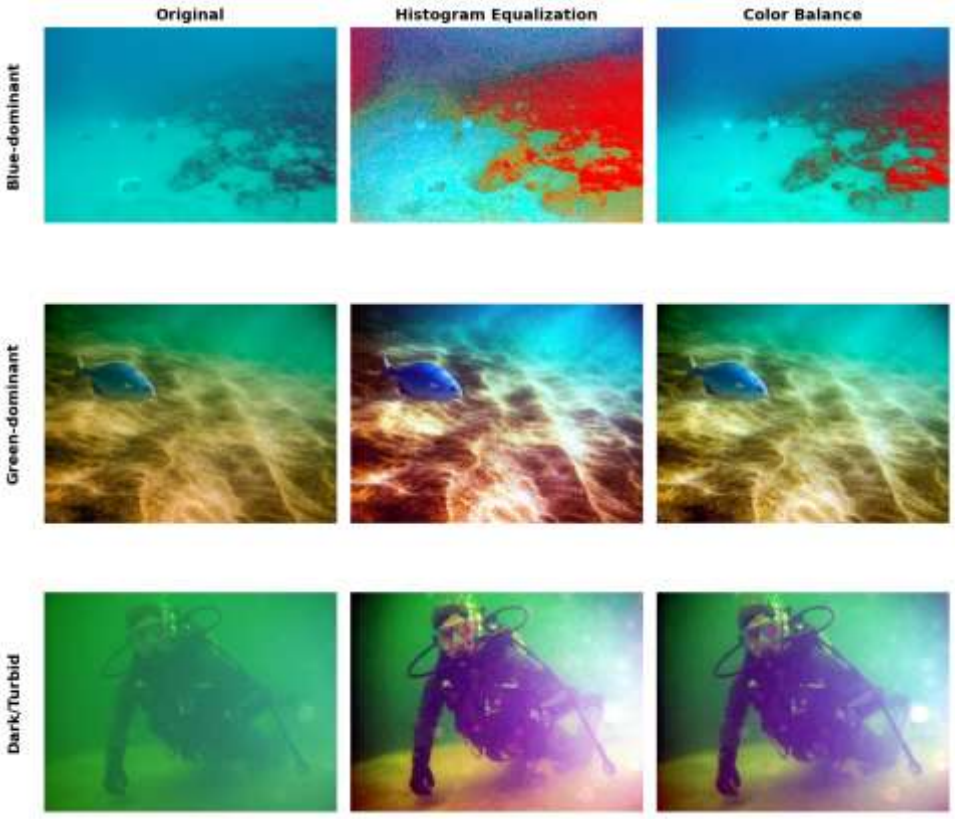


Figure 5. Representative visual comparison per category: original, HE, and Color Balance results.

Blue-dominant images. Figure 5 (top row) shows a generally successful restoration: both HE and Color Balance recovered the natural tan/brown color of the coral and rock formations and the neutral color of the reference chart that were hidden beneath the blue cast in image blue2 (PSNR(CB) = 16.17 dB). However, image blue1 illustrates a specific failure mode of per-channel HE: because the red channel of a deep blue-cast image carries very little usable signal (most red values are crushed near zero), the aggressive full-range stretch performed by HE amplifies the small remaining variation — much of it residual JPEG compression noise — into visible reddish/magenta blotches that are not present in the original scene. This is precisely the kind of red-channel noise-amplification risk that motivated dedicated red-channel restoration methods in the literature [14], and it explains why blue1 has the lowest PSNR(HE) in the blue category (9.04 dB) despite being a comparatively mild degradation case.

Green-dominant images. This category achieved the best overall results in the dataset, including the single highest PSNR(CB) (20.62 dB) and lowest MSE(CB) (563.43) values, obtained on image green2 (Figure 5, middle row). HE recovered vivid red and orange coral coloring that was almost entirely masked by the green cast in the original image, though visibly more saturated than the Color Balance result. The stronger starting balance between the red and blue channels in green-cast water, compared with the near-total loss of red signal in deep blue water, appears to give both methods more legitimate information to work with, which is consistent with the comparatively low residual CCI(CB) of 17.48 observed for this category in Table 3.

Dark/turbid images. This category produced the most heterogeneous outcomes. Image turbid2, a moderately dark but detailed scene, was a clear success for both methods (PSNR(CB) = 18.60 dB), with previously indistinct fish becoming clearly visible after processing. Image turbid1 also showed a substantial visibility improvement, although both methods introduced a noticeable purple/magenta hue shift. Image turbid3, however, is the clearest failure case in the entire dataset: this image is extremely dark and was captured/stored at very low bit depth with heavy block-compression artifacts. Figure 6 shows that its original histogram is a narrow spike concentrated near zero intensity; after HE, this narrow spike is stretched into a sparse, comb-like histogram with large empty gaps, a well-known consequence of applying Histogram Equalization to an image with very few discrete original gray levels. Figure 7 shows the resulting visual output: both HE and Color Balance amplify the underlying compression

ISSN 2986-2337 (Online)

blocks into large, chaotic areas of false color rather than recovering genuine scene detail, and PSNR(HE) collapses to 7.17 dB — the single worst result obtained in this study.

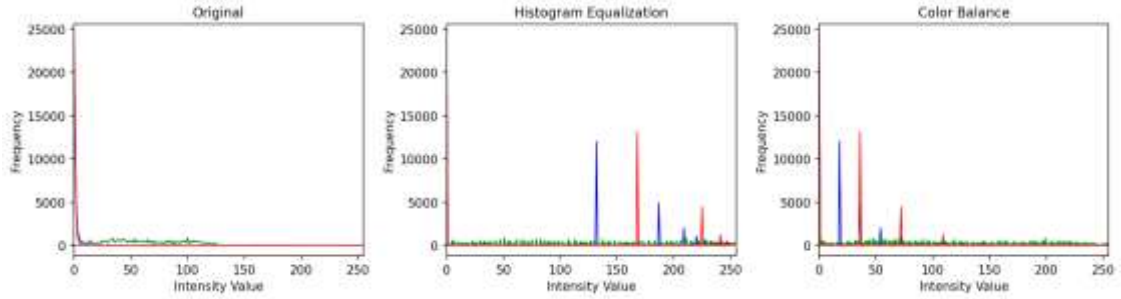


Figure 6. RGB histogram of image turbid3 before and after processing, showing the comb-like spike pattern produced by HE on a narrow, low-bit-depth original histogram.



Figure 7. Visual failure case: image turbid3, the darkest and most heavily compressed image in the dataset.

4.3 Comparative Discussion and Capability Boundary

Taken together, these results indicate a clear trade-off rather than a single best method. HE consistently produces a larger information-theoretic gain (higher entropy, higher contrast) and a stronger numerical reduction of color cast, but this gain is achieved through a more aggressive, higher-magnitude modification of the original pixel values, which carries a correspondingly higher risk of amplifying noise and introducing color artifacts, particularly on images whose red channel or overall bit depth already carries little usable signal. Color Balance, by contrast, is consistently more conservative: it achieved a higher PSNR on all nine images, making it the more reliable default choice when faithfulness to the captured scene is a priority, but its correction of severe color casts is proportionally weaker, as shown by the larger residual CCI observed in the blue-dominant category (31.30) compared with the green-dominant category (17.48).

The clearest capability boundary identified in this study is exposed by image turbid3: both HE and Color Balance perform well on images that retain a reasonably rich underlying intensity distribution, regardless of whether the dominant cast is blue, green, or a moderate degree of haze, but both methods fail once the source image's usable dynamic range has already collapsed through severe under-exposure and heavy compression. This is consistent with a general property of purely spatial-domain contrast enhancement: such methods can only redistribute the intensity information that is already present in the image, and cannot recover detail that was never captured or that was destroyed by prior lossy compression [21]. This observation aligns with Suharyanto and Frieyadie's finding that a more adaptive, locally constrained method (CLAHE) outperformed plain HE and AHE on UIEB images [18], and with Cahyani et al.'s finding that a simple, conservative preprocessing pipeline outperformed more elaborate Retinex and guided-filtering enhancement specifically on the UIEB challenging subset of severely degraded images [22]; both results reinforce the pattern observed here, in which a more conservative correction strategy tends to be more robust than an aggressive, contrast-maximizing one once image quality falls below a certain threshold.

5. Conclusions

This study analyzed the performance of per-channel Histogram Equalization (HE) and the Simplest Color Balance (CB) algorithm on nine real underwater images spanning three degradation categories: blue-dominant, green-dominant, and dark/turbid. Objective evaluation using MSE, PSNR, entropy, RMS contrast, and a color-cast index, together with qualitative visual inspection, showed that Color Balance consistently produced a more faithful result (higher PSNR, lower MSE) on all nine images, while HE produced a larger gain in entropy, contrast, and numerical color-cast reduction but at a higher risk of noise amplification and color artifacts. Both methods performed well on moderately degraded images regardless of whether the dominant cast was blue or green, but both failed on a severely dark, low-bit-depth, heavily compressed image, exposing a clear capability boundary of classical spatial-

ISSN 2986-2337 (Online)

domain restoration: neither method can recover detail that was never captured or that was destroyed by prior compression, since both can only redistribute the intensity information already present in the image.

This study has several limitations that should be considered when interpreting its findings. The dataset consisted of only nine images (three per category), which is sufficient to demonstrate clear and consistent trends but too small to support strong statistical generalization; because no paired radiometric ground truth exists for real-world underwater captures, MSE and PSNR here quantify the magnitude of pixel-level modification relative to the original image rather than restoration accuracy against a known-clean reference; and the Color Balance clip percentage (1%) was fixed rather than optimized per image. Based on these findings, Color Balance is recommended as a safer default choice for practical underwater image restoration pipelines where reliability is a priority, while HE is better suited to images that already retain a reasonably rich intensity distribution across all three channels. For severely degraded images beyond the capability boundary identified in this study, combining these spatial-domain methods with physically motivated preprocessing, such as dark-channel-prior-based dehazing [6], [7] or learning-based enhancement [11], is recommended. Future work should extend this comparison to a larger and more balanced dataset, evaluate adaptive and localized variants such as luminance-channel HE or CLAHE, and incorporate no-reference perceptual metrics such as UIQM [5] and UCIQE [4] for images without an informative pixel-wise reference.

6. Acknowledgment

The author thanks the Faculty of Engineering, Universitas Graha Nusantara, Padangsidimpuan, for institutional support during the preparation of this article.

7. References

[1] C. Li, C. Guo, W. Ren, R. Cong, J. Hou, S. Kwong, and D. Tao, "An underwater image enhancement benchmark dataset and beyond," *IEEE Transactions on Image Processing*, vol. 29, pp. 4376–4389, 2020.

[2] C. O. Ancuti, C. Ancuti, C. De Vleeschouwer, and P. Bekaert, "Color balance and fusion for underwater image enhancement," *IEEE Transactions on Image Processing*, vol. 27, no. 1, pp. 379–393, 2018.

[3] C. Ancuti, C. O. Ancuti, T. Haber, and P. Bekaert, "Enhancing underwater images and videos by fusion," in *Proc. IEEE Conference on Computer Vision and Pattern Recognition (CVPR)*, 2012, pp. 81–88.

[4] M. Yang and A. Sowmya, "An underwater color image quality evaluation metric," *IEEE Transactions on Image Processing*, vol. 24, no. 12, pp. 6062–6071, 2015.

[5] K. Panetta, C. Gao, and S. Agaian, "Human-visual-system-inspired underwater image quality measures," *IEEE Journal of Oceanic Engineering*, vol. 41, no. 3, pp. 541–551, 2016.

[6] K. He, J. Sun, and X. Tang, "Single image haze removal using dark channel prior," *IEEE Transactions on Pattern Analysis and Machine Intelligence*, vol. 33, no. 12, pp. 2341–2353, 2011.

[7] Y.-T. Peng and P. C. Cosman, "Underwater image restoration based on image blurriness and light absorption," *IEEE Transactions on Image Processing*, vol. 26, no. 4, pp. 1579–1594, 2017.

[8] D. Akkaynak and T. Treibitz, "A revised underwater image formation model," in *Proc. IEEE/CVF Conference on Computer Vision and Pattern Recognition (CVPR)*, 2018, pp. 6723–6732.

[9] D. Akkaynak and T. Treibitz, "Sea-thru: A method for removing water from underwater images," in *Proc. IEEE/CVF Conference on Computer Vision and Pattern Recognition (CVPR)*, 2019, pp. 1682–1691.

[10] C.-Y. Li, J.-C. Guo, R.-M. Cong, Y.-W. Pang, and B. Wang, "Underwater image enhancement by dehazing with minimum information loss and histogram distribution prior," *IEEE Transactions on Image Processing*, vol. 25, no. 12, pp. 5664–5677, 2016.

[11] M. J. Islam, Y. Xia, and J. Sattar, "Fast underwater image enhancement for improved visual perception," *IEEE Robotics and Automation Letters*, vol. 5, no. 2, pp. 3227–3234, 2020.

[12] X. Fu and X. Cao, "Underwater image enhancement with global–local networks and compressed-histogram equalization," *Signal Processing: Image Communication*, vol. 86, p. 115892, 2020.

[13] C.-Y. Li, J.-C. Guo, and C.-L. Guo, "Emerging from water: Underwater image color correction based on weakly supervised color transfer," *IEEE Signal Processing Letters*, vol. 25, no. 3, pp. 323–327, 2018.

[14] A. Galdran, D. Pardo, A. Picón, and A. Alvarez-Gila, "Automatic red-channel underwater image restoration," *Journal of Visual Communication and Image Representation*, vol. 26, pp. 132–145, 2015.

[15] N. Limare, J.-L. Lisani, J.-M. Morel, A. B. Petro, and C. Sbert, "Simplest color balance," *Image Processing On Line*, vol. 1, pp. 297–315, 2011.

[16] K. Iqbal, R. A. Salam, A. Osman, and A. Z. Talib, "Underwater image enhancement using an integrated colour model," *IAENG International Journal of Computer Science*, vol. 34, no. 2, 2007.

ISSN 2986-2337 (Online)

[17] Y. Wang, W. Song, G. Fortino, L.-Z. Qi, W. Zhang, and A. Liotta, "An experimental-based review of image enhancement and image restoration methods for underwater imaging," *IEEE Access*, vol. 7, pp. 140233–140251, 2019.

[18] Suharyanto and Frieyadie, "Analisis komparasi perbaikan kualitas citra bawah air berbasis kontras pemerataan histogram," *Jurnal INTI*, vol. 15, no. 1, pp. 95–100, 2020.

[19] S. D. Asri, "Perbaikan kualitas dan kinerja klasifikasi citra bawah air dengan metode CLAHE-CNN," *JSAI: Journal Scientific and Applied Informatics*, vol. 7, no. 1, pp. 182–188, 2024.

[20] W. Song, Y. Wang, D. Huang, A. Liotta, and C. Perra, "Enhancement of underwater images with statistical model of background light and optimization of transmission map," *IEEE Transactions on Broadcasting*, vol. 66, no. 1, pp. 153–169, 2020.

[21] R. C. Gonzalez and R. E. Woods, *Digital Image Processing*, 4th ed. New York: Pearson, 2018.

[22] S. Cahyani, Z. R. Mair, and I. P. Putri, "Evaluasi metode preprocessing sederhana, Retinex, dan guided filtering untuk peningkatan kualitas citra bawah air," *Techno.COM*, vol. 24, no. 3, 2025.

[23] Y. G. Nengsih, K. Samosir, and B. Satria, "Segmentasi pasien rumah sakit berdasarkan pola kunjungan menggunakan algoritma K-Means Clustering untuk optimasi layanan medis," *Jurnal Pendidikan Sains dan Komputer*, vol. 5, no. 1, pp. 59–69, 2025.